Bimolecular Recombination in Organic Photovoltaics

Girish Lakhwani, Akshay Rao, and Richard H. Friend

Cavendish Laboratory, University of Cambridge, Cambridge CB3 0HE, United Kingdom; email: rhf10@cam.ac.uk

Annu. Rev. Phys. Chem. 2014. 65:557–81

First published online as a Review in Advance on January 9, 2014

The *Annual Review of Physical Chemistry* is online at physchem.annualreviews.org

This article's doi: 10.1146/annurev-physchem-040513-103615

Keywords

bulk heterojunction, conjugated polymer, fullerene, charges, Langevin

Abstract

The recombination of electrons and holes is a major loss mechanism in photovoltaic devices that controls their performance. We review scientific literature on bimolecular recombination (BR) in bulk heterojunction organic photovoltaic devices to bring forward existing ideas on the origin and nature of BR and highlight both experimental and theoretical work done to quantify its extent. For these systems, Langevin theory fails to explain BR, and recombination dynamics turns out to be dependent on mobility, temperature, electric field, charge carrier concentration, and trapped charges. Relationships among the photocurrent, open-circuit voltage, fill factor, and morphology are discussed. Finally, we highlight the recent emergence of a molecular-level picture of recombination, taking into account the spin and delocalization of charges. Together with the macroscopic picture of recombination, these new insights allow for a comprehensive understanding of BR and provide design principles for future materials and devices.

1. INTRODUCTION

Over the past decade, the field of organic photovoltaics (OPVs) has made rapid progress, with power conversion efficiencies increasing from 2% to 12% (1–8). These improvements have been driven by a concerted, worldwide research effort, involving numerous disciplines, including physics, chemistry, materials science, and engineering. Excellent progress has been made not only in materials chemistry and device engineering, but also in our understanding of the basic operating principles of these systems. Yet many fundamental questions remain unanswered or controversial, such as the nature and role of morphology and the mechanism of charge generation. In this review, we address perhaps the most pressing question in the field of OPVs, that of charge recombination. Specifically, we discuss the recombination of mobile holes and electrons in bulk heterojunction (BHJ) OPVs, which we term bimolecular recombination (BR) and is also known as nongeminate recombination in the literature (9). As we discuss below, BR ultimately controls the quantum efficiency of OPVs [i.e., the current-voltage (*J-V*) characteristics of the device] (10). Yet it is one of the least understood phenomena, and few strategies to circumvent it have been implemented. We review the relevant concepts in the area and highlight recent research that is beginning to shed light on this extremely important topic.

2. ORGANIC PHOTOVOLTAICS AND THE IMPORTANCE OF BIMOLECULAR RECOMBINATION

2.1. Basic Photophysics in Organic Photovoltaics

The basic structure of an OPV consists of a photoactive layer sandwiched between hole and electron selective contacts (**Figure 1*a***). The photoactive layer comprises a demixed blend of electron donor and electron acceptor semiconductors, referred to as a BHJ (11, 12). **Figure 1*b*** summarizes the basic photophysical process in OPVs (1, 3, 13–16). In step 1, a chromophore in the ground state absorbs a photon that leads to the formation of a tightly bound singlet exciton, owing to the low dielectric constant in organic materials. Singlet excitons are dissociated via charge transfer across the donor-acceptor interface, leading to either long-range charge separation or the formation of bound interfacial charge transfer states (CTS) (step 2 in **Figure 1*b***) (15, 17–22). Such bound charge pairs then decay to the ground state via geminate recombination (step 6 in **Figure 1*b***). Unbound charges, formed after exciton dissociation, can diffuse through the photoactive layer to the hole and electron, extracting contacts. In the current generation of OPVs, hole extraction is accomplished via either PEDOT:PSS [poly(3,4-ethylenedioxythiophene) poly(styrenesulfonate)] or metal oxides such as MoO_x (23, 24), followed by a metal or indium tin oxide. For electron extraction, the metal cathode is often in direct contact with the photoactive layer, although interlayers such as Ca, LiF, and polyelectrolytes (25–28) may be used between the photoactive layer and metal. We return to the role of the contacts below.

2.2. Geminate Versus Bimolecular Recombination

In most BHJ OPVs, soluble fullerene derivatives, such as PCBM ([6,6]-phenyl-C_{61}-butyric acid methyl ester), are ubiquitous electron acceptors. This mainly results from their extreme efficiency at generating free charges following exciton diffusion. Although the reasons for this are still debated within the literature (14, 15, 17, 19, 20, 29–34), it seems clear that it is connected to the availability of delocalized electron states within regions of pure fullerene aggregates. Regardless of the mechanism, in efficient OPVs, exciton dissociation leads to the formation of mostly free charges and greatly reduced geminate recombination. This results in extremely high external

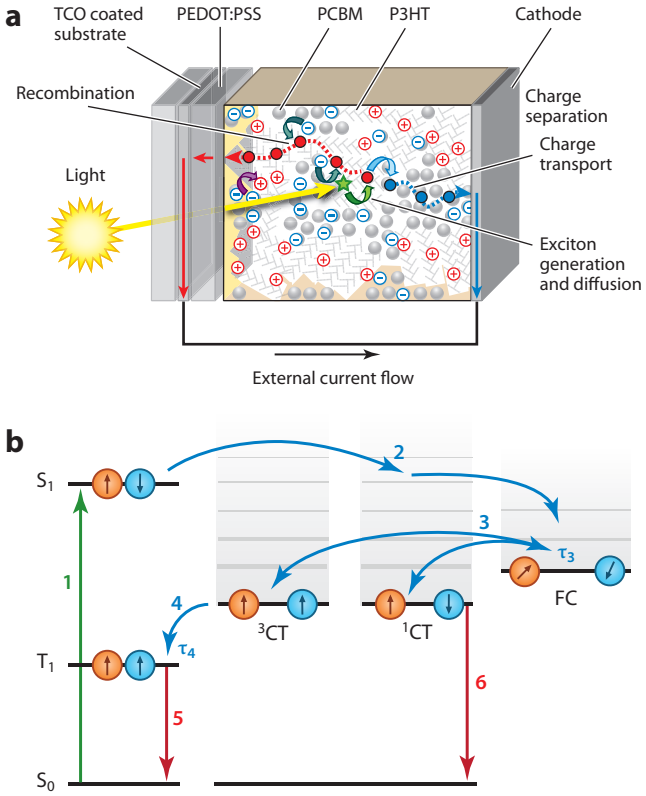

Figure 1

(*a*) Bulk heterojunction organic photovoltaic (OPV) device under operation. Panel *a* reprinted with permission from Reference 10, copyright 2010 by the National Academy of Sciences, USA. Abbreviation: TCO, transparent conductive oxide. (*b*) Photophysical process involved in OPVs. Panel *b* reprinted by permission from Reference 13, copyright Macmillan Publishers Ltd.

quantum efficiencies at short-circuit conditions, often approaching unity (6, 35, 36). Thus, in such devices, geminate recombination is not a significant factor, and bimolecular charge recombination is the main recombination channel (8, 37).

2.3. Morphology, Charge Densities, and the Coulomb Interaction

Pioneering studies by the groups of McGehee (38–40), Russell (41), and DeLongchamp (42) have established that most polymer OPVs comprise nanoscale (<5 nm) domains of pure fullerene and domains of fullerene intimately mixed with the polymer. It is important to note that these length scales are comparable to the Coulomb capture radius (R_C) in organic semiconductors, which can be defined as the length scale at which the Coulomb interaction between the electron and hole is equal to the thermal energy present:

$$R_C = \frac{e^2}{4\pi\varepsilon_0\varepsilon_r kT}. \quad (1)$$

At room temperature ($T = 300$ K), this value can be as large as 16 nm, owing to the low dielectric constant of organics ($\varepsilon_r \approx 3$–4), although considerations of energetic disorder within the system

may reduce this value to 4 nm. The large R_C when coupled with the high charge densities in OPVs under operation, typically 10^{16}–10^{17} charges cm^{-3}, raises the question of why there are not a large number of electron-hole pair encounters before charge extraction at the contacts. And if there are, then why do these not lead to large bimolecular losses in some optimized OPV systems?

2.4. The Importance of Bimolecular Recombination in Organic Photovoltaics

As mentioned above, geminate recombination losses are not very significant in the current generation of OPVs. This means that BR effectively controls *J-V* characteristics of the device; as we move from short-circuit to open-circuit conditions, the charge density within the photoactive layer increases, leading to an increase in BR and a decrease in the fill factor (FF) of the device. The work of Credgington & Durrant (43) demonstrated this elegantly, showing that by limiting the charge density within the photoactive layer and thus the splitting of the quasi-Fermi levels, BR limits the open-circuit voltage (V_{OC}) of the device (see Equation 2). From their analysis using transient photocurrent (TPC) and photovoltage techniques, they demonstrated that V_{OC} follows the following empirical expression:

$$V_{OC} = \frac{1}{e}(IP_D - EA_A) - \frac{\eta kT}{e} \ln\left(\frac{J_{BI}}{J_{SC}}\right), \quad (2)$$

where IP_D, EA_A, η, J_{BI}, and J_{SC} are the ionization potential of the donor, electron affinity of the acceptor, diode ideality factor, nongeminate recombination current, and short-circuit current, respectively. Using measurements of charge densities and decay rates, they reconstructed the *J-V* curve of the device and showed that it was controlled by BR (10) (**Figure 2*a***).

Koster and colleagues (44) studied short-circuit current (J_{SC}) as a function of light intensity (I) for annealed P3HT [poly(3-hexylthiophene)]:PCBM devices at different temperatures. The authors accurately quantified the fraction of charge carriers that recombined (η_{BR}) and established a relationship, $\eta_{BR} = \alpha^{-1} - 1$, based on $J_{SC} \propto I^{\alpha}$. α close to unity signifies the weak influence of BR on the photocurrent. However, for typical polymer:PCBM devices, values significantly lower than 1 are observed. Photocurrent loss, at short circuit, due to BR in a P3HT:PCBM solar cell annealed at 100°C was 17% and was suppressed for devices treated at higher annealing temperatures (see **Figure 2*b***). Several other groups also reached similar conclusions, and there seems to be a general consensus that BR is the major recombination channel within the current generation of OPVs.

2.5. Recombination and the Shockley-Queisser Limit

A point not often considered is the radiative or nonradiative nature of recombination within an OPV. Detailed balance, as discussed in the seminal work of Shockley & Queisser (45), requires that all recombination must be radiative in nature to maximize the V_{OC} of a device. In other words, a perfect solar cell must behave as a perfect light-emitting diode under forward-bias conditions (46). Thus, whether BR occurs via a radiative or nonradiative pathway is an important question. Shockley & Queisser proposed that in inorganic systems, radiative recombination constituted a lower limit to charge carrier recombination. However, the situation in organic systems is different, with inherent disorder within the system and the low dielectric constant not directly yielding free charges, as is the case in inorganic counterparts. The absorbance of energy and the subsequent formation of excitons take place in donor and acceptor phases, whereas electroluminescence comes

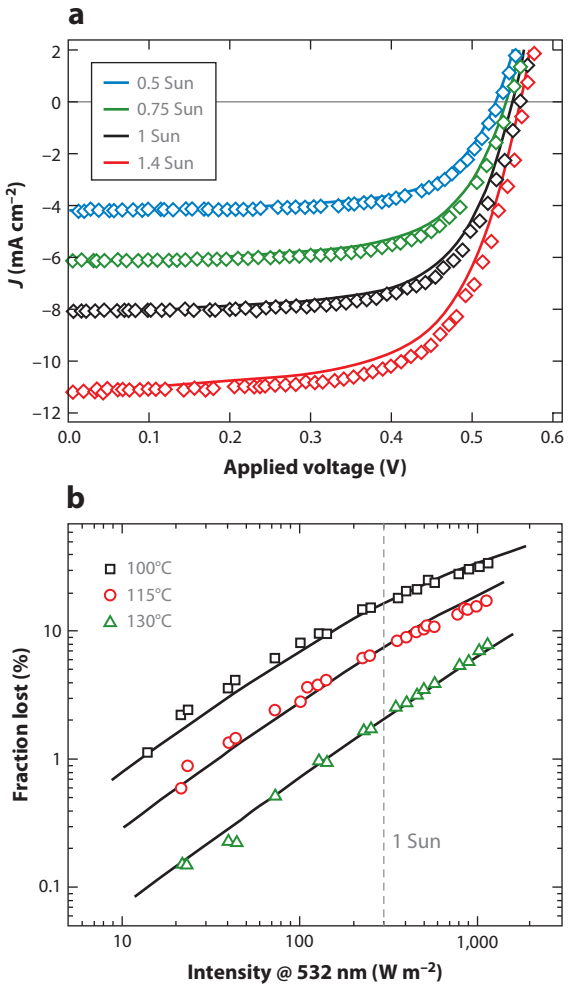

Figure 2

(*a*) Reconstructed (*open symbols*) and experimental (*bold lines*) J-V curves for different light intensities. The reconstructed curve is obtained entirely from the charge carrier density and bimolecular recombination. Panel *a* reprinted with permission from Reference 10, copyright 2010 by the National Academy of Sciences, USA. (*b*) Fits (*solid lines*) to the loss efficiency $\eta_{BR} = 1 - \Delta J^{norm}$ calculated experimentally as a function of white-light illumination for devices annealed at different temperatures. Open symbols are fits to intensity-dependent data for 532-nm light excitation. The dashed line represents light intensity that gives a photocurrent similar to the AM1.5 condition. Panel *b* reprinted with permission from Reference 44, copyright © 2011 Wiley-VCH Verlag GmbH & Co., KGaA, Weinheim.

from the CTS, resulting in absorbance and emission occurring through different energetic states. Consequently, Shockley-Queisser theory was adapted to organic systems (47–50). Vandewal and coworkers (51) showed that for polymer-fullerene OPVs, V_{OC} is related to the absorption and emission of CTS, in accordance with detailed balance. Their work suggests that increasing the quantum efficiency of the radiative recombination of CTS by eliminating nonradiative channels for recombination would increase V_{OC}. However, in reality it is difficult to reach to high efficiencies and V_{OC} in OPVs owing to nonradiative losses.We return to this topic at the end of this review.

3. THEORETICAL UNDERPINNINGS OF BIMOLECULAR RECOMBINATION

Having discussed the basics of OPVs and established the importance of BR above, we now turn to a discussion of its theoretical underpinnings. Many of these theories are derived from previous work on amorphous silicon, with appropriate modifications to deal with the specific properties of organic semiconductors (52, 53).

3.1. Langevin Theory

According to Langevin theory (54) in a three-dimensional system, charge recombination happens when an electron and hole come close to each other, within R_C. BR can be expressed using the Langevin formalism, as shown in Equation 3. In contrast to high-mobility semiconductors, for which direct tunneling recombination is dominant, in disordered low-mobility organic semiconductors, the probability for a recombination event to occur depends on the likelihood of opposite charges finding each other and hence on charge carrier concentrations and the relative mobility at which the opposite charge carriers approach each other. One can understand the relative mobility by assuming that one of the charges is held stationary, with the opposite charge moving with a relative mobility μ equal to the sum of the individual charge carrier mobilities ($\mu = \mu_n + \mu_p$):

$$R = \gamma(np - n_i p_i) \approx \gamma np, \tag{3}$$

$$\gamma = \gamma_{\mathrm{LAN}} = \frac{e\mu}{\varepsilon_0 \varepsilon_r}. \tag{4}$$

Here, n_i and p_i represent intrinsic charge carrier concentrations for electrons n and holes p. Because n_i and p_i are generally smaller, their product is generally smaller than np; hence, they can be neglected, and the equation can be simplified. The prefactor γ is the recombination rate constant. According to Langevin theory, γ can be equated to γ_{LAN}. As shown in Equation 4, γ_{LAN} depends on the dielectric constant of the effective medium, ε_r, and relative mobility term, μ, obtained as the sum of electron (μ_n) and hole (μ_p) mobility.

Equation 3 can also be derived from Debye-Smoluchowski theory (55, 56) assuming the validity of the Einstein relationship $D = \mu kT/e$, where D is the charge diffusion coefficient ($D = D_n + D_p$):

$$\gamma_{\mathrm{SM}} = 4\pi R_C D. \tag{5}$$

Several groups demonstrated the feasibility of Langevin theory in crystalline organic semiconductors. In the mid-1960s and early 1970s, Kepler & Coppage (57), Silver & Sharma (58), and Karl & Sommer (59) studied anthracene single crystals to find a value of γ of the order of 10^{-6} cm^3 s^{-1}. Equation 3 is based on a few assumptions. First, the mean free path for charge carriers has to be smaller than R_C. For disordered organic semiconductors, the values of R_C can be as low as 4 to 5 nm. Disordered semiconductors often have low mobilities, which results in the charge transport being mediated by hopping between energetic sites. Consequently, characteristic hopping lengths, l, and energy dissipation lengths, l_e, due to inelastic scattering are of the order of intersite distances of 1–2 nm, making this assumption fairly satisfied.

The second assumption is that charge carrier transport is homogeneous within the device. As a result, it is assumed that electron and hole densities are nonfluctuating and uncorrelated. This might be true for crystalline semiconductors, for which the mean free path is much larger, averaging out fluctuations and correlations. In low-mobility disordered materials, the electron and hole densities are correlated. For example, Coulomb interaction would modify the mean electron density around a hole. Moreover, because electron and hole densities reside in their

individual components within the donor-acceptor blend, there is a spatial charge distribution. Percolative pathways in BHJ OPVs are responsible for the charge transport of electrons and holes in their individual components. This gives rise to filamentary transport phenomena in which certain transport channels for charges are more active than others, making the charge transport inhomogeneous within the device. Clearly, the second assumption is violated.

Despite the limitations, the Langevin formulism is often employed to describe BR in BHJ OPVs. It is perhaps not surprising that the theoretical predictions using the Langevin expression have failed to explain the contribution of BR determined from experiments on disordered donor-acceptor blends in a typical BHJ OPV device. Given the complications surrounding charge transport in disordered semiconductors, exploring various aspects and dependencies of BR on the performance of devices has been challenging. Enormous experimental and theoretical work has been done to calculate the value of the prefactor γ and quantitatively determine the BR rates.

3.2. Spatially Averaged Mobility

As discussed above, the morphology of the photoactive layer is of great importance as the phase separation between the donor and acceptor determines the spatial profile of charge concentrations and pathways of charge transport. For a recombination event to occur, opposite charges have to reach the donor-acceptor interface, which will depend on their individual mobilities and the profiles of charge concentrations in the respective components. In 1984, Braun (60) proposed a modified γ value to account for the mobility differences between electrons and holes by taking their spatial average:

$$\gamma = \frac{e}{\varepsilon_0 \varepsilon_r} \langle \mu_n + \mu_p \rangle. \tag{6}$$

3.3. Spatial Fluctuation in the Potential Landscape

In 1997, Arkhipov and Adriaenssens (61, 62) proposed a model to calculate BR in disordered semiconductors, which included the effect of both charge spatial profiles and energetic disorder, giving rise to random spatial fluctuations in the potential landscape of disordered semiconductors. Assuming the carrier localization radius to be smaller than the characteristic length of spatial fluctuations and keeping the band gap constant, one can think of the random potential landscape as a profile for the highest occupied molecular orbital (HOMO) and lowest unoccupied molecular orbital (LUMO) with randomly spatially separated maxima and minima in which the charges can localize (see **Figure 3**). The amplitude Δ_E of a potential landscape in an effective medium donor-acceptor blend can be assumed to be the energy difference between either the HOMOs of the donor and acceptor or the LUMOs of the donor and acceptor. In order to recombine, the amplitude of fluctuation acts as the activation barrier, yielding a new term for γ:

$$\gamma = \frac{2\pi \Delta_E}{kT} exp\left(-\frac{2\Delta_E}{kT}\right) \gamma_{\mathrm{LAN}}. \tag{7}$$

We note that in the case of disordered materials, there will be a distribution of Δ_E instead of a single constant value.

3.4. Multiple Trapping

In 2003, Nelson (63) proposed a model for charge recombination in blended OPV systems based on theoretical predictions and transient absorption spectroscopy (TAS) experimental findings on MDMO-PPV (poly[2-methoxy-5-(3,7-dimethyloctyloxy)-1,4-phenylene-vinylene])/PCBM BHJ OPVs as a function of background illumination intensity, temperature, and pump laser intensity.

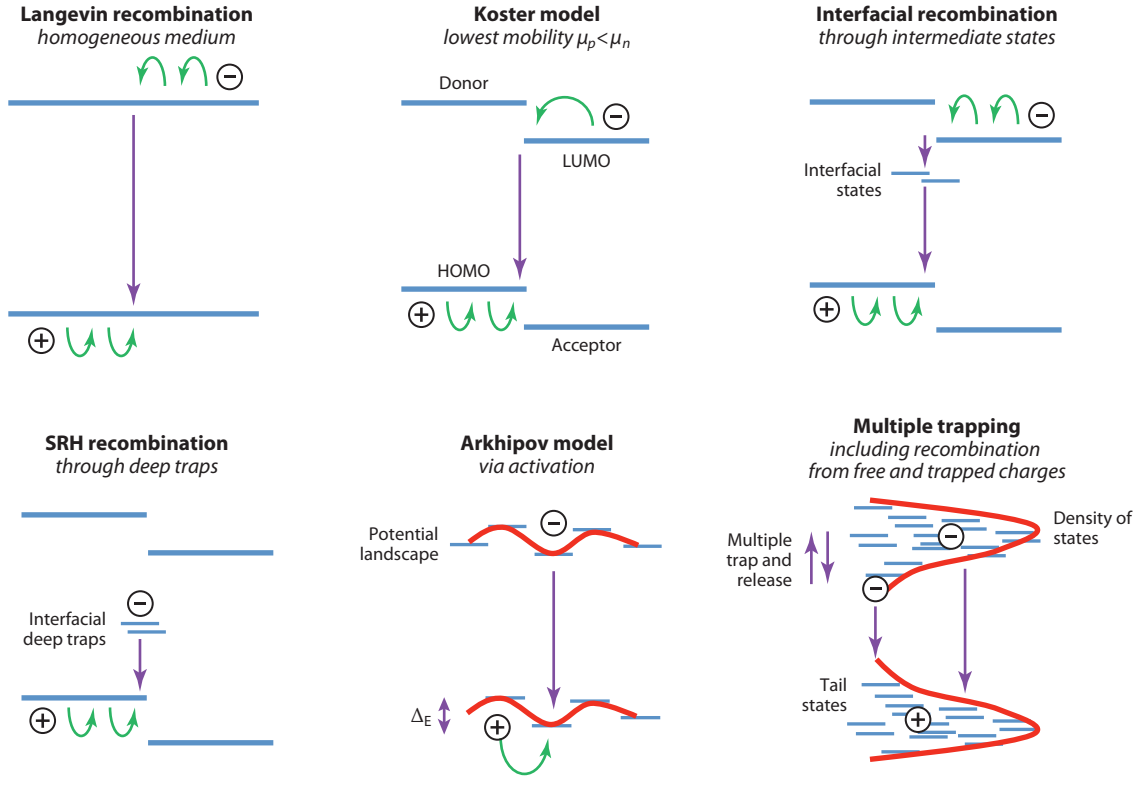

Figure 3

Representation of different bimolecular recombination models. Abbreviations: HOMO, highest occupied molecular orbital; LUMO, lowest unoccupied molecular orbital; SRH, Shockley-Read-Hall.

She proposed that BR is limited by the diffusion of hole polarons toward the PCBM phase, with delayed recombination observed owing to the charge trapping and detrapping of hole polarons, with the hopping between localized states being thermally activated. In the case of a potential landscape comprising deep traps, BR would depend on the detrapping of polarons, making the BR rate proportional to p_{free} instead of p. This leads to the following modification to Equation 3:

$$R = \gamma n p_{\text{free}}. \tag{8}$$

Thus, this model of BR is based on the multiple trapping model of charge transport. Unlike the continuous-time random-walk model (64) for dispersive charge transport, in which charges spend most of the time in trap sites and move between neighboring trap sites, the multiple trapping model (65) is based on the thermal detrapping of charges to free charges before they get trapped again. The reservoir of trapped charges is assumed to be in quasi-equilibrium with the population of free charges, with the detrapping of charges in this case depending exponentially on the trapping energy.

3.5. Slowest Carrier Limited Recombination

In 2006, Koster and colleagues (66) showed that Equation 4 does not hold for polymer/fullerene solar cells, and they put forward another version of γ, which explained their experimental J-V

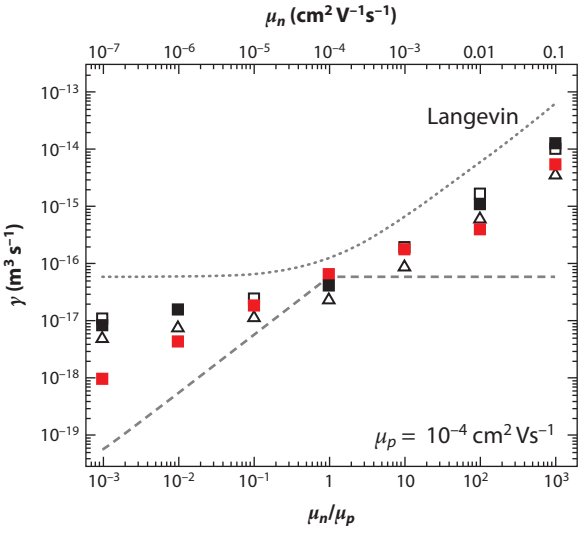

Figure 4

Measured γ value for a 1:1 blend of donor and acceptor polymers using Monte Carlo simulations for an average morphology feature domain size of 4 nm (*black squares*) and 35 nm (*red squares*). Open and closed symbols represent $E = 0$ and 10^7 V m^{-1}, respectively. In all cases, $\mu_n = 10^{-4}$ cm^2 V^{-1}s^{-1}. Dotted and dashed lines show the prediction by the Langevin equation using γ_{LAN} and γ values as proposed by the Koster model, respectively. Figure reprinted with permission from Reference 67, copyright 2008 by the American Physical Society.

characteristics:

$$\gamma = \frac{e}{\varepsilon_0 \varepsilon_r} \min(\mu_n, \mu_p). \tag{9}$$

For opposite charges to meet at the donor-acceptor interface during a recombination event, they argued that the time taken by the slowest charge should be the rate-limiting step (see **Figure 3**). The authors compared their γ values to that proposed by Braun (60), as discussed above. They varied the electron and hole mobilities by annealing P3HT/PCBM devices to obtain a higher mobility mismatch. For higher mobility mismatch, γ obtained by the Braun model would be proportional to a faster carrier, whereas γ from the Koster model would favor the slowest carrier. With the help of drift-diffusion numerical simulations, Koster and colleagues could show that their model represented the experimental *J-V* curves better.

Groves & Greenham (67) performed comparative Monte Carlo simulations on BHJ OPV devices to find γ directly as a function of charge carrier concentration, mobility anisotropy, dimensionality, and the confinement of charge carriers to their respective components. They studied the dependence of mobility mismatch on γ_{LAN} and found γ values in disagreement with the Koster model (**Figure 4**). They proposed that these differences in γ result from the different distances traveled by different charges to the donor-acceptor interface, as charges are spatially distributed.

3.6. Shockley-Read-Hall Recombination

Blom and coworkers (68) took the Koster model (as described above) and incorporated an additional contribution to BR arising from recombination between stationary charges in deep traps and oppositely charged mobile carriers (see **Figure 3**). This additional recombination term was first proposed by Shockley & Read (69). This trap-assisted recombination is often termed

Shockley-Read-Hall (SRH) recombination and is defined by the following expression in Equation 10:

$$R_{\mathrm{SRH}} = \frac{C_n C_p N_t np}{C_n(n+n_1) + C_p(p+p_1)}, \tag{10}$$

$$p_1 n_1 = N_{cv} \exp\left(-\frac{E_{\mathrm{gap}}}{kT}\right) = p_i n_i, \tag{11}$$

$$R_{\mathrm{eff}} = R + R_{\mathrm{SRH}}. \tag{12}$$

Here C_n and C_p are capture cross sections for electrons n and holes p, respectively; E_{gap} is the energy gap ($= IP_{\mathrm{D}} - EA_{\mathrm{A}}$); N_{cv} is the effective density of states; N_t is the density of electron traps; and $n_1 p_1$ follow the relationship shown in Equation 11 under equilibrium conditions. In the case of SRH recombination, the rate of recombination turns out to be monomolecular in nature (n/τ).

3.7. Image Charge Effect

Szmytkowski (70) considered the influence of polarization effects caused by a charge close to the donor-acceptor interface of different permittivities. As a result, charge e in one dielectric medium (ε_1) sees an opposite image charge in the other medium ($\varepsilon_2 > \varepsilon_1$) and is attracted toward it. He argued that this is analogous to the metal-semiconductor case in which the Coulombic interaction between the charge in the organic semiconductor and the opposite image charge in the metal with much larger permittivity causes extraction current (71): A similar occurrence in donor-acceptor blends would result in a possible recombination current. Here the recombination current is treated as a result of the movement of a charge carrier (μ_1) toward the donor-acceptor interface owing to Coulombic attraction from its image; it is not supposed to be interpreted as recombination between a charge carrier and its image. Szmytkowski argued that this process would compete with BR, leading to a reduction of Langevin-type recombination. As a result, he proposed a new γ term, which is less than γ_{LAN}:

$$\gamma = \left|\frac{\varepsilon_1 - \varepsilon_2}{\varepsilon_1 + \varepsilon_2}\right| \frac{e\mu_1}{\varepsilon_0 \varepsilon_1}. \tag{13}$$

3.8. The Role of Intermediates in the Recombination Process

In all the above theories, based on the Langevin formalism, electron-hole recombination occurs when the distance between charges, R_1, is zero. The role of an intermediate species that may form below R_C but before recombination has not been considered. Based on the Smoluchowski-Collins-Kimball approach (55, 72), in 2010 Hilczer & Tachiya (73) proposed a unified theory for geminate and nongeminate recombination and defined γ taking into consideration BR occurring at a nonzero distance with an intrinsic recombination rate, p_R ($= k_{\mathrm{BET}} R_1$), related to the back-electron transfer rate, k_{BET}, between the electron and hole separated by R_1. Detailed derivations can be found in their paper. The ratio between γ and γ_{LAN} in the absence of an electric field is

$$\frac{\gamma}{\gamma_{\mathrm{LAN}}} = \frac{1}{1 - e^{-R_C/R_1} + \frac{DR_C}{p_R R_1^2} e^{-R_C/R_1}}, \tag{14}$$

whereas the ratio between the diffusion coefficient, D, and p_R is

$$\frac{D}{p_R} = A \exp\left(-\frac{\Delta E}{kT}\right). \tag{15}$$

Here A is $D_{\text{inf}}/p_{R\text{inf}}$, and ΔE ($= \Delta E_D - \Delta E_p$) is the difference between the activation energy of D and p_R. We note that at the limit $R_1 \to 0$, the $\gamma/\gamma_{\text{LAN}}$ ratio approaches 1, giving rise to the classical Langevin expression.

As can be seen from the discussion in the above section, there has been considerable progress in the theoretical treatment of BR over the past 20 years. Newer theories, taking into account the complex properties of BHJ OPVs, are meeting with greater success in explaining experimental results. However, much work still remains to build a comprehensive picture of recombination.

4. RECOMBINATION DYNAMICS

Having discussed the theoretical background for BR, we now turn to the key experimental findings regarding recombination dynamics. The determination of γ using transient electro-optical techniques such as TAS, transient photovoltage, and photo-CELIV (photoinduced current and charge extraction by linearly increasing voltage) in blended films and devices allowed researchers to investigate BR independent of other additional charge carrier losses often observed in J-V data, via shunts, recombination at electrodes, and geminate recombination. However, attempts to quantify these findings based on the models described above have met with only limited success.

4.1. Charge Transport Measurements

Österbacka and coworkers (74, 75) used time-of-flight, double-injection CELIV techniques to study BHJ OPVs of regioregular P3HT:PCBM and MDMO-PPV:PCBM. For P3HT:PCBM, they found γ to be orders of magnitude lower than that predicted by Langevin expression. They concluded that this resulted from the microcrystalline ordered morphology, which results in spatially separated charge transport pathways for electrons and holes. They also proposed that the ordered morphology resulted in two-dimensional transport via lamellar P3HT structures (76). The effect of dimensional constraints on BR was studied previously for organic light-emitting diode (OLED) devices (77) accounting for experimentally observed γ to be lower than predicted by Langevin expression. However, for MDMO-PPV:PCBM, Österbacka and coworkers (78) found that the BR rate could be described reasonably by the Langevin expression, the difference with P3HT:PCBM being the lack of an ordered microcrystalline morphology.

4.2. Charge Carrier Decay Measurements

In 2008, Durrant and coworkers (79, 80) experimentally determined the rate law for charge carrier decay in thermally annealed P3HT:PCBM (1:1) devices using TAS, TPC, and transient photovoltage techniques to probe charge carrier lifetimes and V_{OC} as a function of light intensity. Assuming the charge generation rate to be constant within the device, one can define the charge carrier decay rates (for $n \approx p$) within the device as shown in Equation 16:

$$\frac{\partial n}{\partial t} \propto -\gamma n^2 \propto n^{\delta}, \tag{16}$$

$$\frac{\partial n}{\partial t} \propto -\frac{n^{\lambda-1}}{(1+\lambda)\tau_{\Delta n0} n_0^{\lambda}} n^2, \tag{17}$$

$$\gamma = \frac{n^{\lambda-1}}{(1+\lambda)\tau_{\Delta n0} n_0^{\lambda}}. \tag{18}$$

Here δ is the order of the decay of charge carriers. The values of $\tau_{\Delta n0}$ and λ ($=\omega/\rho$) are determined by studying the dependence of the charge carrier lifetime, $\tau_{\Delta n}$ [$=\tau_{\Delta n0}\exp(-\omega V_{OC})$], and charge carrier concentration, n [$=n_0\exp(\rho V_{OC})$], on V_{OC}, through intensity-dependent transient photovoltage and TPC measurements.

Durrant and coworkers (79) showed that charge carrier decay dynamics followed a higher-order dependence on charge carrier concentration, as expressed in Equation 17 with λ values between 1.5 and 2.5. They found λ to be sensitive to device preparation conditions, consistent with the observed range of values. This was the first time strong charge carrier dependence on charge carrier lifetimes was proposed for P3HT:PCBM devices, making γ no longer a constant parameter but instead dependent on charge carrier concentration, $\gamma(n)$ (Equation 18).

This interpretation is equivalent to that proposed by Nelson (63), as discussed in Section 3.4, who stated that nonlinear dispersive bimolecular decay dynamics occurs through localized trap states, maintaining a quasi-equilibrium between mobile and trapped charges. As a result, BR was found to be dependent on the detrapping of charges. Furthermore, using charge extraction techniques, Durrant and coworkers (81) showed that dark current in annealed P3HT:PCBM devices also exhibited charge carrier density dependence similar to that found in devices under illumination, as discussed above. They proposed that the dark current in these devices originated entirely from the BR.

McNeill and coworkers (82, 83) and Street and coworkers (84, 85) studied the interplay between trapping and detrapping rates for SRH recombination while reproducing their intensity- and bias-dependent TPC experiments. Cowan et al. (86) deliberately introduced traps and defect states within the devices and showed increased SRH recombination using TAS and *J-V* measurements.

4.3. Temperature-Dependent Measurements

Deibel and coworkers (87, 88) studied temperature dependence in pristine and annealed P3HT:PCBM devices using the photo-CELIV technique. In pristine devices, they observed a reduced recombination rate, with the reduction factor $\zeta = \gamma/\gamma_{LAN}$ being mostly temperature independent. Surprisingly, for annealed devices at room temperature, the authors found ζ of the order of 10^{-4}. For such low values of γ, BR was deemed to not be the limiting factor for device performance. Importantly, for annealed P3HT:PCBM devices, ζ was found to increase with decreasing temperature, similar to observations by Juška et al. (89). This observation is opposite to predictions from the Arkhipov or Koster model (**Figure 5*a***). Juška et al. (89) also investigated the electric field dependence of ζ, only to find a weak correlation, suggesting that BR is not caused by tunneling. The authors proposed that this resulted from a reduced Coulombic interaction between opposite charges at the donor-acceptor interface; however, the precise reason was unclear. Hilczer & Tachiya (73) explained the results (see **Figure 5*b***) based on their own model (see Section 3.8). They argued that the similar negative values of ΔE obtained for both data sets indicate that the activation energy of the intrinsic recombination parameter p_R is larger than that of the diffusion constant, D (see Equation 15), making the process controlled by the recombination of charges when they are at a finite close distance, rather than on their approach to find each other via diffusion (73). The ΔE values obtained in these cases are not very different from values obtained from Marcus theory.

Deibel and coworkers (88) further suggested that the BR rate should incorporate the spatial dependence of charge carrier concentrations rather than spatially averaged concentrations of the same. With the help of numerical simulations, they fit the experimental data as shown in **Figure 5*a*** and proposed that γ should depend on temperature, electric field, and charge carrier density, expressing the reduction factor ζ as $\zeta(T, E, G)$. Here G is the charge generation rate. Furthermore,

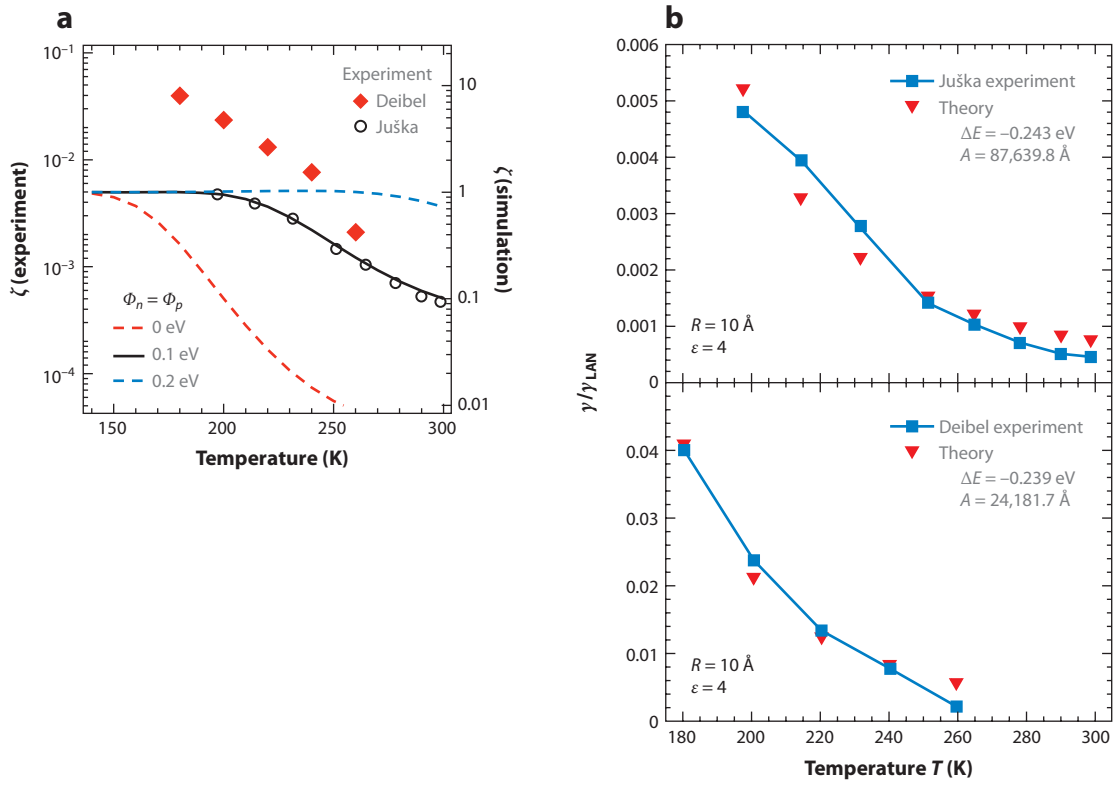

Figure 5

(*a*) Temperature-dependent ζ ($=\gamma/\gamma_{\mathrm{LAN}}$) values obtained experimentally by Deibel and coworkers (88) using the photo-CELIV (photoinduced current and charge extraction by linearly increasing voltage) technique (*symbols*) and values obtained via macroscopic simulation for symmetric devices with different injection barriers, φ (*dashed and solid lines*). The fit obtained for the case $\varphi = 0.1$ eV (*solid line*) involves both contributions: dynamic $\zeta(T, E, G)$ as proposed and a static ζ based on the Szmytkowski expression (Equation 13). Panel *a* reprinted with permission from Reference 88, copyright 2009 by the American Physical Society. (*b*) Temperature-dependent $\gamma/\gamma_{\mathrm{LAN}}$ values obtained by Hilczer & Tachiya (73) using their unified model (*inverse triangles*), which fit the experimental data (*squares*) nicely. Panel *b* reprinted with permission from Reference 73, copyright 2010 American Chemical Society.

they explained the higher-order charge decay as being influenced by the trapping of charges in the tail states of Gaussian density of states. As a result, a weaker dependence of γ on the charge carrier concentration can be expected at higher temperatures, at which detrapping due to disorder becomes unimportant. At lower temperatures, the majority of charges would stay trapped, showing a greater dependence of γ on charge decay.

4.4. Mobility-Dependent Measurements

From the discussion above, the dependence of γ on the charge carrier concentration (n) is clear. As it is known that the charge carrier mobility (μ) is also dependent on n (90–92), it is important to establish the dependence of γ on μ. In 2010, Durrant and coworkers (93) found through independent measurements on the same device of P3HT:PCBM that the dependence of γ and μ on n was self-consistent [$\gamma(n) \propto \mu(n) \propto n^{0.35}$] (**Figure 6*a***). This finding was instrumental in defining that the fundamental origin of both γ and μ is the same and originates from the trapping and detrapping of charges.

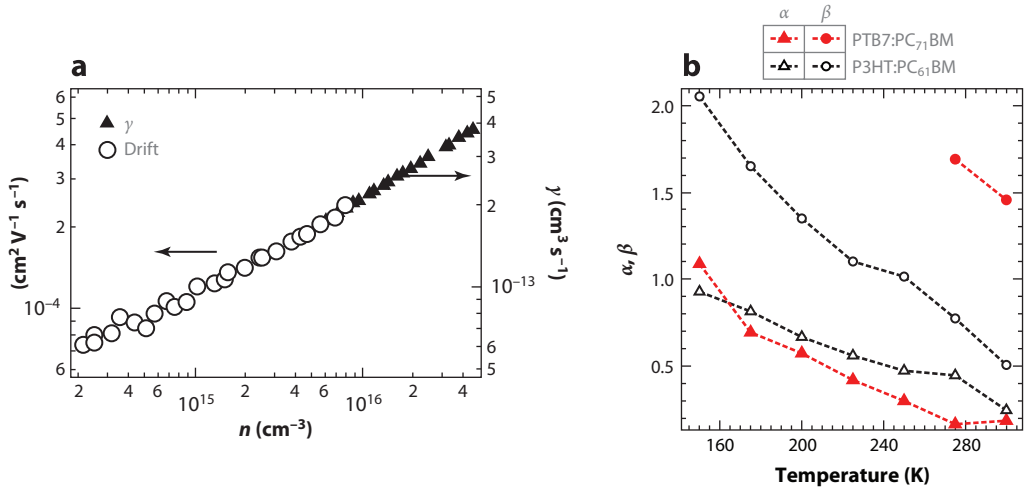

Figure 6

(*a*) Comparison of drift carrier mobility (*left vertical axis*) and γ value (*right vertical axis*) dependence on the charge carrier density, n. Panel *a* reprinted with permission from Reference 93, copyright © 2010 Wiley-VCH Verlag GmbH & Co., KGaA, Weinheim. (*b*) Values of α and β as a function of temperature for different polymer:PCBM blends. Panel *b* reprinted with permission from Reference 94, copyright © 2012 Wiley-VCH Verlag GmbH & Co., KGaA, Weinheim.

Deibel and coworkers (94) also found a similar relationship between $\mu(n)$ ($\propto n^{\alpha}$) and $\gamma(n)$ ($\propto n^{\beta}$) but extended it to different temperatures for two different polymer:PCBM devices (**Figure 6*b***). They considered recombination ($\propto n^{\beta+2}$) a sum of recombination between free charges and recombination between trapped charges and mobile charges. They pointed out that the effect of trapping is more pronounced in P3HT:PCBM at low temperatures and that higher effective disorder (σ/kT) results in slower detrapping of charges, yielding higher recombination orders.

4.5. Reaction Orders and Ideality Factors

Transient optical techniques such as TAS, photo-CELIV, TPC, and charge extraction probe all charges within the polymer/PCBM films and devices defining the order of charge carrier decay (δ),

$$\left[\frac{\partial n}{\partial t}\right]_T \propto n^{\delta}, \tag{19}$$

whereas steady-state J-V techniques probe free charges with charge decay order Δ,

$$\left[\frac{\partial n}{\partial t}\right]_{SS} \propto n_{free}^{\Delta}. \tag{20}$$

For example, in a typical Langevin-based BR, $\Delta = 2$ indicates a bimolecular nature of decay, whereas in the case of monomolecular SRH recombination, $\Delta = 1$. For intermediate cases in which both BR and SRH recombination are important, Δ is found to be between 1 and 2. For a similar intermediate case, the order of the reaction $\delta > 2$ was determined through transient optical techniques. However, other experiments and numerical simulations might be required to determine the dominant loss mechanism within BR and SRH recombination in these intermediate cases (95–97). It is hence important to reconcile orders of decay derived from both kinds of experiments. The diode ideality factor determined from charge carrier concentration–dependent studies of V_{OC} from J-V measurements gives a good indication of the nature of recombination.

Establishing a relationship between the ideality factor and order of charge decay would be helpful in understanding the underlying dynamics from steady-state measurements.

Kirchartz & Nelson (98) established a link between δ and Δ and also gave an expression relating δ and η:

$$\Delta = (\delta - 1)^{-1} + 1, \tag{21}$$

$$\delta = \frac{m}{\eta}, \tag{22}$$

$$m = \frac{2E_{cb}}{kT}. \tag{23}$$

Here E_{cb} is the slope of the tail of the density of states. The authors showed that the shape of the density of states affects the ideality factors. For the case of shallower traps or trap-free transport ($\eta = 1$), the tail slope is less than kT, yielding values of m close to 2, as calculated from Equation 22. This would yield $\delta = 2$, as expected from Langevin theory. With a slope higher than kT in the case of deeper traps, δ would become greater than 2.

Deibel and coworkers (99) formulated an alternate expression:

$$\Delta = \frac{2}{\eta}. \tag{24}$$

With the help of charge extraction and J-V measurements on P3HT/PCBM devices, they related the influence of oxygen exposure on δ, Δ, and η. They showed that for annealed P3HT:PCBM BHJ OPVs, the dominant recombination is between mobile charges and trapped charges in the tail states, with Δ values close to 1.7. Increased exposure to oxygen allowed for the formation of trap sites. As a result, J-V measurements followed both monomolecular (SRH; $\Delta = 1$) and bimolecular (BR; $\Delta = 2$) kinetics to give values for Δ between 1 and 2. Together with $1 < \Delta < 2$, $\eta > 1$ and $\delta > 2$ indicate dominant SRH recombination. Thus, using the above relationships, one can determine the type of recombination from just the J-V curve.

4.6. Space-Charge Limited Dynamics

Blom and coworkers (100) reported low FFs in PCPDTBT/PCBM BHJ OPVs, even though charge transport is balanced, with similar μ_n and μ_p. They argued that low FFs originated from the intimately mixed nanomorphology of the donor-acceptor blend, which resulted in geminate losses and recombination limited current, showing square root dependence on the effective applied voltage, linear dependence on the light intensity, and a constant saturation voltage.

The square root dependence of the photocurrent on the effective applied voltage has been explained by Goodman & Rose (101) and is a signature of both the space-charge limited current and recombination limited current. However, both these effects can be differentiated by intensity-dependent measurements (102). Low-mobility disordered semiconductor devices always compete with BR for charge extraction. For a longer lifetime of charges, τ, the distance traveled by charges is greater than the thickness of the film; hence most charges are extracted. This case is generally prevalent in coarse phase-separated blends. However, in intimately mixed blends, the lifetime is lower, and charges recombine before being extracted, making the device recombination limited, with the photocurrent following the dynamics

$$J_{\text{ph}} = qG\sqrt{\mu_{p(n)}\tau_{p(n)}}\sqrt{V}. \tag{25}$$

However, if there is a difference between μ_n and μ_p, the space charge would start to accumulate, changing the internal electric field. At higher intensities, this would make the device full of space charge. Under such a regime, the photocurrent would become space-charge limited, with the photocurrent following the dynamics

$$J_{\text{ph}} \leq (qG)^{0.75} \left(\frac{9}{8}\varepsilon_0 \varepsilon \mu_{\text{slowest}}\right)^{0.25} \sqrt{V}. \tag{26}$$

Tessler & Rappaport argued that at high intensities, BR could well arise as a result of the space-charge limited current, with the slowest charge carrier setting the photocurrent (103, 104).

4.7. Relation Between Bimolecular Recombination and Solar Cell Properties

There seems to be an overall consensus that the values of γ measured experimentally are one to four orders of magnitude lower than those for γ_{LAN}. However, as discussed above, different interpretations have emerged, viewing the reduced recombination rates as a result of the spatial separation of charges (61), image charge effects (70), energetic disorder (67, 105, 106), trap states (63, 105, 107, 108), carriers with slowest transit to the donor-acceptor interface (66), dimensional constraints (76, 77, 109), lateral and vertical charge transport (110), and intrinsic recombination rate (73). In all these competing interpretations, the morphology of the photoactive layer plays a key role. Numerous studies, some discussed above, have attempted to investigate the recombination dynamics while manipulating the morphology via techniques such as thermal annealing (44, 87, 107, 111, 112), doping (111, 113), and processing via the use of solvent additives (114–116). Various donor and acceptor materials, both crystalline and noncrystalline, have also been studied (117–125).

Credgington & Durrant (43) established a relationship between V_{OC} and the FF with the recombination rate, which allowed for accurate reconstruction of the device J-V curves. Koster and colleagues (44) established a relationship between the photocurrent and the diode ideality factor to determine the magnitude of BR. Blom and coworkers (126) were also able to show that in all BHJ OPVs, the number of electron traps is the same, as high as 10^{23} m^{-3}, and the traps are all located at the reduction potential of the oxygen water complex at approximately 3.6 eV. Assuming $n \approx p$, and with only electron trapping active (i.e., $C_n \gg C_p$ and $\mu_n = 0$), they further showed that SRH recombination depends primarily on the mobility of the mobile carrier and can be expressed analogous to the Langevin formalism (127):

$$R_{\text{SRH}} = C_p N_t p = \frac{q}{\varepsilon} \mu_p N_t p. \tag{27}$$

Deibel and colleagues (94) reached a similar conclusion. Thus, good progress has been made with these empirical models that can be said to operate at a macroscopic level, with correlations being drawn to the microscopic properties of materials. However, key shortcomings remain within all these models, which we explore below.

5. THE ROLE OF CONTACTS

In all the above discussions, we deal with the properties of the photoactive layer of the OPV and how they affect BR. However, charge-extracting contacts also play a large role in OPVs (128, 129). Within all BR models, there is competition between the extraction of charges at the electrode and recombination within the photoactive layer. Investigators have thought of the time taken for extraction as being controlled by the drift and diffusion of charge carriers to the contacts (i.e., entirely controlled by photoactive layer properties). However, Kumar et al. (130) recently showed that modification of the electrode properties can have significant effects on the extraction rate. Comparing PTB7:PCBM solar cells with PEDOT:PSS as the hole extracting contact, they

found that the rate of hole extraction at short circuit increased by a factor of seven when the PEDOT:PSS/photoactive layer interface was modified with MeOH, without changing the photoactive layer properties. This dramatic improvement in extraction shows that even in relatively efficient devices, the photoactive layer/contact interface, and not the bulk of the photoactive layer, can control the rate of charge extraction and hence the rate of BR.

6. THE ROLE OF SPIN AND DELOCALIZATION

In this section, we move from a macroscopic to a molecular view of recombination and review recent results highlighting the importance of spin and delocalization to BR.

6.1. Recombination in Organic Light-Emitting Diodes

Previous sections discuss attempts to describe recombination in OPVs within the Langevin framework. The emphasis on Langevin dynamics is based partly on the success of this model at explaining recombination dynamics in OLEDs (131, 132). OLEDs are a more mature field, in comparison to OPVs, and it is natural that attempts were made to apply models for recombination in OLEDs to OPVs. However, a key element of recombination in OLEDs, that of spin, has been entirely neglected in OPVs until recently.

In OLEDs, electrons and holes are injected into the device at opposite electrodes and move into the photoactive layer, in which they recombine to form excitons. As the spins of the injected charges are uncorrelated, recombination gives spin singlets and spin triplets in a 1:3 ratio dictated by spin statistics (133–135). Thus, the importance of the spins of recombining charges has long been recognized in OLEDs, with the formation of these nonradiative triplets a key performance bottleneck, and much effort has been made to overcome this problem (136–139).

6.2. Spin-Dependent Recombination in Organic Photovoltaics

In OPVs, the BR of charges implicitly means that there is no spin correlation between the electron and hole. However, in contrast to OLEDs, the spin of recombining charges has not been taken into account in any of the models discussed above. In addition, the role of intermediate states formed following electron-hole encounters, which may act as precursors to recombination, has hardly been considered.

Recently, it has been established that spin does in fact play a crucial role during recombination in OPVs, as in OLEDs. Using TAS, Rao et al. (13) demonstrated that BR leads to the formation of triplet excitons in some polymer:fullerene blends. These triplet excitons are then annihilated by charges in the blend (step 5 of **Figure 1*b***), meaning that their formation is a terminal loss process.

6.3. Charge Transfer States and Delocalization

Importantly, the demonstration that triplet excitons can be formed via BR suggests that intermediate CTS play an important role in mediating recombination. This is perhaps not surprising as CTS mediate the initial exciton dissociation and charge separation process (15). Crucially, CTS are known to play a role in OLEDs, for which emission from exciplex-like states has been observed and is the operation mechanism of some OLEDs. Thus BR in OPVs should lead to the formation of spin singlet and spin triplet CTS, ^{1}CT and ^{3}CT, in a 1:3 ratio as required by spin statistics (step 3 in **Figure 1*b***). The ^{1}CT states can recombine to the ground state (step 6 of **Figure 1*b***), but the recombination of ^{3}CT to the ground state is spin forbidden. This leads to the creation of a spin blockade of recombination (13).

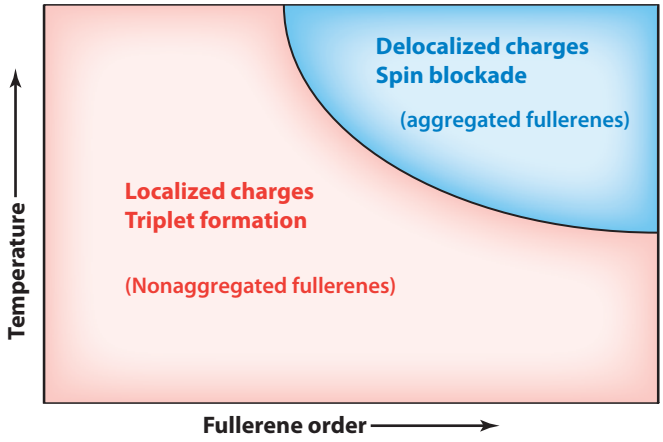

Figure 7

Triplet phase diagram for polymer:fullerene bulk heterojunction organic photovoltaic devices, illustrating the effect of temperature on the existence of polymer triplets and the extent of charge delocalization for varying fullerene order.

In most OPV blends, the molecular triplet (T_1) on the donor lies energetically below the CTS, as is required to maximize V_{OC}. In such cases, the ^{3}CT state can relax to T_1 (step 4 of **Figure 1*b***). Rao et al. (13) confirmed the mechanism by the detection of T_1, formed via BR in polymer:fullerene blends. However, triplet excitons were not detected in a blend with ordered PCBM aggregates, only in blends with disordered PCBM or other fullerenes such as ICMA and ICBA, which, unlike PCBM, do not crystallize. At lower temperatures, BR was found to lead to the formation of triplets, even in the blend with ordered PCBM aggregates. This suggests that there is a thermally activated pathway that competes with the relaxation of ^{3}CT to T_1. This pathway was considered to be the dissociation of ^{3}CT back to free charges (step 3 in **Figure 1*b***). In the blend with ordered PCBM aggregates, this process outcompetes the relaxation of ^{3}CT to T_1. However, in the blends with disordered PCBM, ICMA, or ICBA, this process cannot outcompete the relaxation of ^{3}CT to T_1.

This dissociation of ^{3}CT back to free charges in ordered blends was explained in terms of delocalization of the charge wave functions. For the ordered fullerene blends, such as PCBM, this delocalization will be larger, lowering the binding energy of the CTS and making the thermal activation back to free charges easier. Thus, fullerene aggregation plays a crucial role in BR, allowing for CTS to be recycled back to free charges. Hence, in most OPV blends, with low fullerene content or disordered fullerene domains, BR will lead to the formation of triplet excitons. This is the major recombination channel in current OPVs (**Figure 7**).

However, these findings also mean that not all electron-hole capture events lead to terminal recombination. In optimized blends, which always contain domains of aggregated fullerene, the recombination rate can be greatly suppressed owing to the spin blockade of recombination, which helps explain how OPVs can give such high quantum efficiencies despite having nanoscale morphologies and high charge densities. This also goes some way in explaining why measured rates of recombination are orders of magnitude less than the theoretical Langevin rate, as discussed above.

Interestingly, the blocking of recombination to triplets is also important with regard to V_{OC}. As discussed above, detailed balance requires that recombination must proceed radiatively to maximize V_{OC} (45–51). Recombination to triplets is a nonradiative decay channel, which means it lowers the maximum attainable V_{OC}. However, if ordered fullerene domains are present (**Figure 7**),

recombination to triplets is blocked, forcing all recombination to proceed via ^{1}CT, a radiative decay channel. This in turn will allow for higher V_{OC}. More research into the role of spin and delocalization is clearly needed as these results provide important design insights on how to block recombination in OPVs.

7. CONCLUDING REMARKS

As highlighted in this review, our understanding of BR has made great progress over the past decade. BR is now widely accepted to be the main recombination channel in BHJ OPVs. This is largely a result of extensive experimental studies of recombination dynamics in OPV, undertaken via transient electro-optical techniques and careful studies and modeling of *J-V* curves. These studies have also been successful at establishing relationships between BR and several important OPV properties, such as V_{OC}, FFs, and diode ideality factors. Theoretically, starting with the Langevin formalism, interpretations have been more nuanced to take into account the unique properties of BHJ OPVs, such as structural and energetic disorder, low mobility, traps, and blend morphology. Given these complexities, it is not surprising that these theories are still evolving and do not provide a quantitative picture of recombination dynamics. However, they still provide a good framework to consider the processes involved, at a qualitative level. Finally, a new molecular-level picture of recombination is emerging from time-resolved photophysical studies, one that takes into account the charge carrier spin and delocalization of wave functions. When combined with macroscopic models, this should allow for a more complete picture of recombination, as well as provide design principles on how to minimize recombination-induced losses.

SUMMARY POINTS

1. BR is the most important recombination channel in current BHJ OPVs, controlling the *J-V* curve and limiting V_{OC} and FFs.
2. The theoretical understanding of BR has made good progress, although it still cannot fully explain the observed experimental results. Current theories also do not consider a full molecular-level picture; rather, they are confined to macroscopic parameters. This ultimately limits their usefulness in providing design rules for future materials and devices.
3. Experimental studies of recombination have been successful in establishing relationships between BR and BHJ OPV parameters. These allow for a thorough analysis of where losses are occurring within a device, based on just a simple *J-V* measurement.
4. A molecular-level picture of BR, taking into account the spin and delocalization of charge carriers, is in a nascent stage and shows great promise.

DISCLOSURE STATEMENT

The authors are not aware of any affiliations, memberships, funding, or financial holdings that might be perceived as affecting the objectivity of this review.

ACKNOWLEDGMENTS

The authors thank Dr. Dan Credgington, Dr. Stavros Athanasapoulos, and Prof. Neil C. Greenham for valuable discussions.

LITERATURE CITED

1. Brabec C, Gowrisanker S, Halls J, Laird D, Jia S, Williams S. 2010. Polymer-fullerene bulk-heterojunction solar cells. *Adv. Mater.* 22:3839–56
2. Dennler G, Scharber MC, Brabec CJ. 2009. Polymer-fullerene bulk-heterojunction solar cells. *Adv. Mater.* 21:1323–38
3. Dennler G, Scharber MC, Ameri T, Denk P, Forberich K, et al. 2008. Design rules for donors in bulk-heterojunction tandem solar cells towards 15% energy-conversion efficiency. *Adv. Mater.* 20:579–83
4. Brabec C, Scherf U, Dyakonov V, eds. 2008. *Organic Photovoltaics: Materials, Device Physics, and Manufacturing Technologies*. New York: Wiley
5. Scharber MC, Mühlbacher D, Koppe M, Denk P, Waldauf C, et al. 2006. Design rules for donors in bulk-heterojunction solar cells: towards 10% energy-conversion efficiency. *Adv. Mater.* 18:789–94
6. Li G, Zhu R, Yang Y. 2012. Polymer solar cells. *Nat. Photon.* 6:153–61
7. Chen L-M, Hong Z, Li G, Yang Y. 2009. Recent progress in polymer solar cells: manipulation of polymer:fullerene morphology and the formation of efficient inverted polymer solar cells. *Adv. Mater.* 21:1434–49
8. Liang Y, Xu Z, Xia J, Tsai S-T, Wu Y, et al. 2010. For the bright future: bulk heterojunction polymer solar cells with power conversion efficiency of 7.4%. *Adv. Mater.* 22:E135–38
9. Credgington D, Hamilton R, Atienzar P, Nelson J, Durrant JR. 2011. Non-geminate recombination as the primary determinant of open-circuit voltage in polythiophene:fullerene blend solar cells: an analysis of the influence of device processing conditions. *Adv. Funct. Mater.* 21:2744–53
10. Shuttle CG, Hamilton R, O'Regan BC, Nelson J, Durrant JR. 2010. Charge-density-based analysis of the current–voltage response of polythiophene/fullerene photovoltaic devices. *Proc. Natl. Acad. Sci. USA* 107:16448–52
11. Halls JJM, Walsh CA, Greenham NC, Marseglia EA, Friend RH, et al. 1995. Efficient photodiodes from interpenetrating polymer networks. *Nature* 376:498–500
12. Yu G, Gao J, Hummelen JC, Wudl F, Heeger AJ. 1995. Polymer photovoltaic cells: enhanced efficiencies via a network of internal donor-acceptor heterojunctions. *Science* 270:1789–91
13. Rao A, Chow PCY, Gélinas S, Schlenker CW, Li C-Z, et al. 2013. The role of spin in the kinetic control of recombination in organic photovoltaics. *Nature* 500:435–39
14. Brédas J-L, Norton JE, Cornil J, Coropceanu V. 2009. Molecular understanding of organic solar cells: the challenges. *Acc. Chem. Res.* 42:1691–99
15. Bakulin A, Rao A, Pavelyev V, van Loosdrecht P, Pshenichnikov M, et al. 2012. The role of driving energy and delocalized states for charge separation in organic semiconductors. *Science* 335:1340–44
16. Friend R, Phillips M, Rao A, Wilson M, Li Z, McNeill C. 2012. Excitons and charges at organic semiconductor heterojunctions. *Faraday Discuss.* 155:339–48
17. Grancini G, Maiuri M, Fazzi D, Petrozza A, Egelhaaf HJ, et al. 2013. Hot exciton dissociation in polymer solar cells. *Nat. Mater.* 12:29–33
18. Veldman D, Meskers SCJ, Janssen RAJ. 2009. The energy of charge-transfer states in electron donor–acceptor blends: insight into the energy losses in organic solar cells. *Adv. Funct. Mater.* 19:1939–48
19. Deibel C, Strobel T, Dyakonov V. 2010. Role of the charge transfer state in organic donor-acceptor solar cells. *Adv. Mater.* 22:4097–111
20. Jailaubekov A, Willard AP, Tritsch JR, Chan W-L, Sai N, et al. 2013. Hot charge-transfer excitons set the time limit for charge separation at donor/acceptor interfaces in organic photovoltaics. *Nat. Mater.* 12:66–73
21. Zhu XY, Yang Q, Muntwiler M. 2009. Charge-transfer excitons at organic semiconductor surfaces and interfaces. *Acc. Chem. Res.* 42:1779–87
22. McGehee MD. 2009. Organic solar cells: overcoming recombination. *Nat. Photon.* 3:250–52
23. Sun Y, Takacs C, Cowan S, Seo J, Gong X, et al. 2011. Efficient, air-stable bulk heterojunction polymer solar cells using MoO_x as the anode interfacial layer. *Adv. Mater.* 23:2226–30
24. Vaynzof Y, Kabra D, Zhao L, Ho PKH, Wee ATS, Friend RH. 2010. Improved photoinduced charge carriers separation in organic-inorganic hybrid photovoltaic devices. *Appl. Phys. Lett.* 97:033309

25. Liu X, Wen W, Bazan G. 2012. Post-deposition treatment of an arylated-carbazole conjugated polymer for solar cell fabrication. *Adv. Mater.* 24:4505–10
26. Seo JH, Gutacker A, Sun Y, Wu H, Huang F, et al. 2011. Improved high-efficiency organic solar cells via incorporation of a conjugated polyelectrolyte interlayer. *J. Am. Chem. Soc.* 133:8416–19
27. He Z, Zhong C, Su S, Xu M, Wu H, Cao Y. 2012. Enhanced power-conversion efficiency in polymer solar cells using an inverted device structure. *Nat. Photon.* 6:591–95
28. He Z, Zhong C, Huang X, Wong W-Y, Wu H, et al. 2011. Simultaneous enhancement of open-circuit voltage, short-circuit current density, and fill factor in polymer solar cells. *Adv. Mater.* 23:4636–43
29. Etzold F, Howard I, Mauer R, Meister M, Kim T-D, et al. 2011. Ultrafast exciton dissociation followed by nongeminate charge recombination in PCDTBT:PCBM photovoltaic blends. *J. Am. Chem. Soc.* 133:9469–79
30. Bakulin AA, Dimitrov SD, Rao A, Chow PCY, Nielsen CB, et al. 2013. Charge-transfer state dynamics following hole and electron transfer in organic photovoltaic devices. *J. Phys. Chem. Lett.* 4:209–15
31. Jamieson FC, Domingo EB, McCarthy-Ward T, Heeney M, Stingelin N, Durrant JR. 2012. Fullerene crystallisation as a key driver of charge separation in polymer/fullerene bulk heterojunction solar cells. *Chem. Sci.* 3:485–92
32. Dimitrov S, Bakulin A, Nielsen C, Schroeder B, Du J, et al. 2012. On the energetic dependence of charge separation in low-band-gap polymer/fullerene blends. *J. Am. Chem. Soc.* 134:18189–92
33. Clarke TM, Durrant JR. 2010. Charge photogeneration in organic solar cells. *Chem. Rev.* 110:6736–67
34. Ohkita H, Cook S, Astuti Y, Duffy W, Tierney S, et al. 2008. Charge carrier formation in polythiophene/fullerene blend films studied by transient absorption spectroscopy. *J. Am. Chem. Soc.* 130:3030–42
35. Park SH, Roy A, Beaupre S, Cho S, Coates N, et al. 2009. Bulk heterojunction solar cells with internal quantum efficiency approaching 100%. *Nat. Photon.* 3:297–302
36. Price S, Stuart A, Yang L, Zhou H, You W. 2011. Fluorine substituted conjugated polymer of medium band gap yields 7% efficiency in polymer-fullerene solar cells. *J. Am. Chem. Soc.* 133:4625–31
37. Credgington D, Durrant JR. 2012. Insights from transient optoelectronic analyses on the open-circuit voltage of organic solar cells. *J. Phys. Chem. Lett.* 3:1465–78
38. Hoke ET, Sachs-Quintana IT, Lloyd MT, Kauvar I, Mateker WR, et al. 2012. The role of electron affinity in determining whether fullerenes catalyze or inhibit photooxidation of polymers for solar cells. *Adv. Energy Mater.* 2:1351–57
39. Mayer AC, Michael FT, Shawn RS, Jonathan R, Christoph JB, et al. 2009. Bimolecular crystals of fullerenes in conjugated polymers and the implications of molecular mixing for solar cells. *Adv. Funct. Mater.* 19:1173–79
40. Cates NC, Gysel R, Beiley Z, Miller CE, Toney MF, et al. 2009. Tuning the properties of polymer bulk heterojunction solar cells by adjusting fullerene size to control intercalation. *Nano Lett.* 9:4153–57
41. Liu F, Gu Y, Jung JW, Jo WH, Russell TP. 2012. On the morphology of polymer-based photovoltaics. *J. Polymer Sci. B* 50:1018–44
42. Hammond MR, Kline RJ, Herzing AA, Richter LJ, Germack DS, et al. 2011. Molecular order in high-efficiency polymer/fullerene bulk heterojunction solar cells. *ACS Nano* 5:8248–57
43. Credgington D, Durrant JR. 2012. Insights from transient optoelectronic analyses on the open-circuit voltage of organic solar cells. *J. Phys. Chem. Lett.* 3:1465–78
44. Koster LJA, Kemerink M, Wienk MM, Maturová K, Janssen RAJ. 2011. Quantifying bimolecular recombination losses in organic bulk heterojunction solar cells. *Adv. Mater.* 23:1670–74
45. Shockley W, Queisser HJ. 1961. Detailed balance limit of efficiency of *p-n* junction solar cells. *J. Appl. Phys.* 32:510–19
46. Miller OD, Yablonovitch E, Kurtz SR. 2012. Strong internal and external luminescence as solar cells approach the Shockley-Queisser limit. *IEEE J. Photovolt.* 2:303–11
47. Giebink NC, Wiederrecht GP, Wasielewski MR, Forrest SR. 2010. Ideal diode equation for organic heterojunctions. I. Derivation and application. *Phys. Rev. B* 82:155305
48. Giebink NC, Lassiter BE, Wiederrecht GP, Wasielewski MR, Forrest SR. 2010. Ideal diode equation for organic heterojunctions. II. The role of polaron pair recombination. *Phys. Rev. B* 82:155306
49. Koster LJA, Shaheen SE, Hummelen JC. 2012. Pathways to a new efficiency regime for organic solar cells. *Adv. Energy Mater.* 2:1246–53

50. Rau U. 2007. Reciprocity relation between photovoltaic quantum efficiency and electroluminescent emission of solar cells. *Phys. Rev. B* 76:085303
51. Vandewal K, Tvingstedt K, Gadisa A, Inganas O, Manca J. 2009. On the origin of the open-circuit voltage of polymer-fullerene solar cells. *Nat. Mater.* 8:904–9
52. Schiff EA. 1995. Diffusion-controlled bimolecular recombination of electrons and holes in a-Si:H. *J. Non-Cryst. Solids* 190:1–8
53. Jackson WB. 1989. Role of bimolecular recombination in picosecond photoinduced absorption of hydrogenated amorphous silicon. *Philos. Mag. Lett.* 60:277–82
54. Langevin P. 2013. Recombinaison et mobilites des ions dans les gaz. *Ann. Chim. Phys.* 28:433–530
55. Smoluchowski MV. 1917. Versuch einer mathematischen Theorie der Koagulationskinetik kolloider Loeschungen. *Z. Phys. Chem.* 92:129
56. Debye P. 1942. Reaction rates in ionic solution. *J. Electrochem. Soc.* 82:265–72
57. Kepler RG, Coppage FN. 1966. Generation and recombination of holes and electrons in anthracene. *Phys. Rev.* 151:610–14
58. Silver M, Sharma R. 1967. Carrier generation and recombination in anthracene. *J. Chem. Phys.* 46:692–96
59. Karl N, Sommer G. 1971. Field dependent losses of electrons and holes by bimolecular volume recombination in the excitation layer of anthracene single crystals studied by drift current pulses. *Phys. Status Solidi A* 6:231–41
60. Braun CL. 1984. Electric field assisted dissociation of charge transfer states as a mechanism of photocarrier production. *J. Chem. Phys.* 80:4157–61
61. Adriaenssens GJ, Arkhipov VI. 1997. Non-Langevin recombination in disordered materials with random distributions. *Solid State Commun.* 103:541–43
62. Arkhipov VI, Adriaenssens GJ. 1997. Kinetics of low temperature charge carrier recombination. *J. Phys. Condens. Matter* 9:6869–76
63. Nelson J. 2003. Diffusion-limited recombination in polymer-fullerene blends and its influence on photocurrent collection. *Phys. Rev. B* 67:155209
64. Scher H, Montroll E. 1975. Anomalous transit-time dispersion in amorphous solids. *Phys. Rev. B* 12:2455–77
65. Schmidlin F. 1977. Theory of trap-controlled transient photoconduction. *Phys. Rev. B* 16:2362–85
66. Koster LJA, Mihailetchi VD, Blom PWM. 2006. Bimolecular recombination in polymer/fullerene bulk heterojunction solar cells. *Appl. Phys. Lett.* 88:052104
67. Groves C, Greenham NC. 2008. Bimolecular recombination in polymer electronic devices. *Phys. Rev. B* 78:155205
68. Mandoc MM, Kooistra FB, Hummelen JC, Boer BD, Blom PWM. 2007. Effect of traps on the performance of bulk heterojunction organic solar cells. *Appl. Phys. Lett.* 91:263505
69. Shockley W, Read WT Jr. 1952. Statistics of the recombination of holes and electrons. *Phys. Rev.* 87:835–42
70. Szmytkowski J. 2009. Analysis of the image force effects on the recombination at the donor-acceptor interface in organic bulk heterojunction solar cells. *Chem. Phys. Lett.* 470:123–25
71. Scott JC, Malliaras GG. 1999. Charge injection and recombination at the metal–organic interface. *Chem. Phys. Lett.* 299:115–19
72. Collins FC, Kimball GE. 1949. Diffusion controlled reaction rates. *J. Colloid Sci.* 4:425–37
73. Hilczer M, Tachiya M. 2010. Unified theory of geminate and bulk electron-hole recombination in organic solar cells. *J. Phys. Chem. C* 114:6808–13
74. Pivrikas A, Juška G, Mozer AJ, Scharber M, Arlauskas K, et al. 2005. Bimolecular recombination coefficient as a sensitive testing parameter for low-mobility solar-cell materials. *Phys. Rev. Lett.* 94:176806
75. Juška G, Genevičius K, Sliaužys G, Nekrašas N, Österbacka R. 2008. Double injection in organic bulk heterojunction. *J. Non-Cryst. Solids* 354:2858–61
76. Juška G, Genevičius K, Nekrašas N, Sliaužys G, Österbacka R. 2009. Two dimensional Langevin recombination in regioregular poly(3-hexylthiophene). *Appl. Phys. Lett.* 95:013303
77. Greenham NC, Bobbert PA. 2003. Two-dimensional electron-hole capture in a disordered hopping system. *Phys. Rev. B* 68:245301

78. Pivrikas A, Sariciftci NS, Juška G, Österbacka R. 2007. A review of charge transport and recombination in polymer/fullerene organic solar cells. *Prog. Photovolt.* 15:677–96
79. Shuttle CG, O'Regan B, Ballantyne AM, Nelson J, Bradley DDC, et al. 2008. Experimental determination of the rate law for charge carrier decay in a polythiophene:fullerene solar cell. *Appl. Phys. Lett.* 92:093311
80. Shuttle CG, O'Regan B, Ballantyne AM, Nelson J, Bradley DDC, Durrant JR. 2008. Bimolecular recombination losses in polythiophene:fullerene solar cells. *Phys. Rev. B* 78:113201
81. Shuttle CG, Maurano A, Hamilton R, O'Regan B, Mello JCD, Durrant JR. 2008. Charge extraction analysis of charge carrier densities in a polythiophene/fullerene solar cell: analysis of the origin of the device dark current. *Appl. Phys. Lett.* 93:183501
82. Hwang I, McNeill CR, Greenham NC. 2009. Drift-diffusion modeling of photocurrent transients in bulk heterojunction solar cells. *J. Appl. Phys.* 106:094506
83. Li Z, Lakhwani G, Greenham NC, McNeill CR. 2013. Voltage-dependent photocurrent transients of PTB7:PC_{70}BM solar cells: experiment and numerical simulation. *J. Appl. Phys.* 114:034502
84. Street RA. 2011. Localized state distribution and its effect on recombination in organic solar cells. *Phys. Rev. B* 84:075208
85. Cowan SR, Street RA, Cho S, Heeger AJ. 2011. Transient photoconductivity in polymer bulk heterojunction solar cells: competition between sweep-out and recombination. *Phys. Rev. B* 83:035205
86. Cowan SR, Leong WL, Banerji N, Dennler G, Heeger AJ. 2011. Identifying a threshold impurity level for organic solar cells: enhanced first-order recombination via well-defined PC_{84}BM traps in organic bulk heterojunction solar cells. *Adv. Funct. Mater.* 21:3083–92
87. Deibel C, Baumann A, Dyakonov V. 2008. Polaron recombination in pristine and annealed bulk heterojunction solar cells. *Appl. Phys. Lett.* 93:163303
88. Deibel C, Wagenpfahl A, Dyakonov V. 2009. Origin of reduced polaron recombination in organic semiconductor devices. *Phys. Rev. B* 80:075203
89. Juška G, Arlauskas K, Stuchlik J, Österbacka R. 2006. Non-Langevin bimolecular recombination in low-mobility materials. *J. Non-Cryst. Solids* 352:1167–71
90. Coehoorn R, Pasveer W, Bobbert P, Michels M. 2005. Charge-carrier concentration dependence of the hopping mobility in organic materials with Gaussian disorder. *Phys. Rev. B* 72:155206
91. Bouhassoune M, van Mensfoort SLM, Bobbert PA, Coehoorn R. 2009. Carrier-density and field-dependent charge-carrier mobility in organic semiconductors with correlated Gaussian disorder. *Org. Electron.* 10:437–45
92. Pasveer WF, Cottaar J, Tanase C, Coehoorn R, Bobbert PA, et al. 2005. Unified description of charge-carrier mobilities in disordered semiconducting polymers. *Phys. Rev. Lett.* 94:206601
93. Shuttle CG, Hamilton R, Nelson J, O'Regan BC, Durrant JR. 2010. Measurement of charge-density dependence of carrier mobility in an organic semiconductor blend. *Adv. Funct. Mater.* 20:698–702
94. Rauh D, Deibel C, Dyakonov V. 2012. Charge density dependent nongeminate recombination in organic bulk heterojunction solar cells. *Adv. Funct. Mater.* 22:3371–77
95. Street RA, Schoendorf M, Roy A, Lee JH. 2010. Interface state recombination in organic solar cells. *Phys. Rev. B* 81:205307
96. Deibel C, Wagenpfahl A. 2010. Comment on "Interface state recombination in organic solar cells." *Phys. Rev. B* 82:207301
97. Street RA. 2010. Reply to "Comment on 'Interface state recombination in organic solar cells.'" *Phys. Rev. B* 82:207302
98. Kirchartz T, Nelson J. 2012. Meaning of reaction orders in polymer:fullerene solar cells. *Phys. Rev. B* 86:165201
99. Deibel C, Rauh D, Foertig A. 2013. Order of decay of mobile charge carriers in P3HT:PCBM solar cells. *Appl. Phys. Lett.* 103:043307
100. Lenes M, Morana M, Brabec CJ, Blom PWM. 2009. Recombination-limited photocurrents in low bandgap polymer/fullerene solar cells. *Adv. Funct. Mater.* 19:1106–11
101. Goodman AM, Rose A. 1971. Double extraction of uniformly generated electron-hole pairs from insulators with noninjecting contacts. *J. Appl. Phys.* 42:2823–30

102. Mihailetchi VD, Wildeman J, Blom PWM. 2005. Space-charge limited photocurrent. *Phys. Rev. Lett.* 94:126602
103. Tessler N, Rappaport N. 2004. Excitation density dependence of photocurrent efficiency in low mobility semiconductors. *J. Appl. Phys.* 96:1083–87
104. Rappaport N, Solomesch O, Tessler N. 2005. The interplay between space charge and recombination in conjugated polymer/molecule photocells. *J. Appl. Phys.* 98:033714
105. Kirchartz T, Pieters BE, Kirkpatrick J, Rau U, Nelson J. 2011. Recombination via tail states in polythiophene:fullerene solar cells. *Phys. Rev. B* 83:115209
106. Albrecht U, Bässler H. 1995. Langevin-type charge carrier recombination in a disordered hopping system. *Phys. Status Solidi B* 191:455–59
107. Bartelt JA, Beiley ZM, Hoke ET, Mateker WR, Douglas JD, et al. 2013. The importance of fullerene percolation in the mixed regions of polymer-fullerene bulk heterojunction solar cells. *Adv. Energy Mater.* 3:364–74
108. Yang X, Wang RZ, Wang YC, Sheng CX, Li H, et al. 2013. Long lived photoexcitation dynamics in π-conjugated polymer and fullerene blended films. *Org. Electron.* 14:2058–64
109. Nenashev AV, Jansson F, Baranovskii SD, Österbacka R, Dvurechenskii AV, Gebhard F. 2010. Role of diffusion in two-dimensional bimolecular recombination. *Appl. Phys. Lett.* 96:213304
110. Maturová K, van Bavel SS, Wienk MM, Janssen RAJ, Kemerink M. 2009. Morphological device model for organic bulk heterojunction solar cells. *Nano Lett.* 9:3032–37
111. Street RA, Krakaris A, Cowan SR. 2012. Recombination through different types of localized states in organic solar cells. *Adv. Funct. Mater.* 22:4608–19
112. Yang XN, Loos J, Veenstra SC, Verhees WJH, Wienk MM, et al. 2005. Nanoscale morphology of high-performance polymer solar cells. *Nano Lett.* 5:579–83
113. Armin A, Juška G, Philippa BW, Burn PL, Meredith P, et al. 2013. Doping-induced screening of the built-in-field in organic solar cells: effect on charge transport and recombination. *Adv. Energy Mater.* 3:321–27
114. Lee JK, Ma WL, Brabec CJ, Yuen J, Moon JS, et al. 2008. Processing additives for improved efficiency from bulk heterojunction solar cells. *J. Am. Chem. Soc.* 130:3619–23
115. Albrecht S, Schindler W, Kurpiers J, Kniepert J, Blakesley JC, et al. 2012. On the field dependence of free charge carrier generation and recombination in blends of PCPDTBT/PC_{70}BM: influence of solvent additives. *J. Phys. Chem. Lett.* 3:640–45
116. Peet J, Kim JY, Coates NE, Ma WL, Moses D, et al. 2007. Efficiency enhancement in low-bandgap polymer solar cells by processing with alkane dithiols. *Nat. Mater.* 6:497–500
117. Westenhoff S, Howard IA, Hodgkiss JM, Kirov KR, Bronstein HA, et al. 2008. Charge recombination in organic photovoltaic devices with high open-circuit voltages. *J. Am. Chem. Soc.* 130:13653–58
118. Sánchez-Díaz A, Izquierdo M, Filippone S, Martin N, Palomares E. 2010. The origin of the high voltage in DPM12/P3HT organic solar cells. *Adv. Funct. Mater.* 20:2695–700
119. Massip S, Oberhumer PM, Tu G, Albert-Seifried S, Huck WTS, et al. 2011. Influence of side chains on geminate and bimolecular recombination in organic solar cells. *J. Phys. Chem. C* 115:25046–55
120. Proctor CM, Kim C, Neher D, Nguyen T-Q. 2013. Nongeminate recombination and charge transport limitations in diketopyrrolopyrrole-based solution-processed small molecule solar cells. *Adv. Funct. Mater.* 23:3584–94
121. Maurano A, Hamilton R, Shuttle CG, Ballantyne AM, Nelson J, et al. 2010. Recombination dynamics as a key determinant of open circuit voltage in organic bulk heterojunction solar cells: a comparison of four different donor polymers. *Adv. Mater.* 22:4987–92
122. Li W, Hendriks KH, Roelofs WSC, Kim Y, Wienk MM, Janssen RAJ. 2013. Efficient small bandgap polymer solar cells with high fill factors for 300 nm thick films. *Adv. Mater.* 25:3182–86
123. Kyaw AKK, Wang DH, Gupta V, Leong WL, Ke L, et al. 2013. Intensity dependence of current-voltage characteristics and recombination in high-efficiency solution-processed small-molecule solar cells. *ACS Nano* 7:4569–77
124. Howard IA, Laquai F, Keivanidis PE, Friend RH, Greenham NC. 2009. Perylene tetracarboxydiimide as an electron acceptor in organic solar cells: a study of charge generation and recombination. *J. Phys. Chem. C* 113:21225–32

125. Di Nuzzo D, Wetzelaer G-JAH, Bouwer RKM, Gevaerts VS, Meskers SCJ, et al. 2013. Simultaneous open-circuit voltage enhancement and short-circuit current loss in polymer:fullerene solar cells correlated by reduced quantum efficiency for photoinduced electron transfer. *Adv. Energy Mater.* 3:85–94
126. Nicolai HT, Kuik M, Wetzelaer GAH, Boer BD, Campbell C, et al. 2012. Unification of trap-limited electron transport in semiconducting polymers. *Nat. Mater.* 11:882–87
127. Kuik M, Koster LJA, Wetzelaer GAH, Blom PWM. 2011. Trap-assisted recombination in disordered organic semiconductors. *Phys. Rev. Lett.* 107:256805
128. Chen LM, Xu Z, Hong Z, Yang Y. 2010. Interface investigation and engineering: achieving high performance polymer photovoltaic devices. *J. Mater. Chem.* 20:2575–98
129. Graetzel M, Janssen R, Mitzi D, Sargent E. 2012. Materials interface engineering for solution-processed photovoltaics. *Nature* 488:304–12
130. Kumar A, Lakhwani G, Elmalem E, Huck WTS, Rao A, et al. 2014. Interface limited charge extraction and recombination in organic photovoltaics. Submitted manuscript
131. Wallikewitz BH, Kabra D, Gelinas S, Friend RH. 2012. Triplet dynamics in fluorescent polymer light-emitting diodes. *Phys. Rev. B* 85:045209
132. Kabra D, Lu L, Song M, Snaith H, Friend R. 2010. Efficient single-layer polymer light-emitting diodes. *Adv. Mater.* 22:3194–98
133. Köhler A, Wilson JS, Friend RH. 2002. Fluorescence and phosphorescence in organic materials. *Adv. Mater.* 14:701–7
134. Friend RH, Gymer RW, Holmes AB, Burroughes JH, Marks RN, et al. 1999. Electroluminescence in conjugated polymers. *Nature* 397:121–28
135. Köhler A, Bässler H. 2009. Triplet states in organic semiconductors. *Mater. Sci. Eng. R* 66:71–109
136. Uoyama H, Goushi K, Shizu K, Nomura H, Adachi C. 2012. Highly efficient organic light-emitting diodes from delayed fluorescence. *Nature* 492:234–38
137. Goushi K, Yoshida K, Sato K, Adachi C. 2012. Organic light-emitting diodes employing efficient reverse intersystem crossing for triplet-to-singlet state conversion. *Nat. Photon.* 6:253–58
138. Segal M, Singh M, Rivoire K, Difley S, Van Voorhis T, Baldo MA. 2007. Extrafluorescent electroluminescence in organic light-emitting devices. *Nat. Mater.* 6:374–78
139. Baldo MA, O'Brien DF, You Y, Shoustikov A, Sibley S, et al. 1998. Highly efficient phosphorescent emission from organic electroluminescent devices. *Nature* 395:151–54

Annual Review of
Physical Chemistry
Volume 65, 2014

Contents

Indexes

Errata

An online log of corrections to *Annual Review of Physical Chemistry* articles may be found at http://www.annualreviews.org/errata/physchem